

## Accepted Article

**Title:** The Catalytic Properties of Copper-based Nanoscale Coordination Polymer Fabricated by Solvent-Etching Top-Down Route

**Authors:** Qiang Ju, Xiaowei Cao, Wei Huang, and Zhenlan Fang

This manuscript has been accepted after peer review and appears as an Accepted Article online prior to editing, proofing, and formal publication of the final Version of Record (VoR). This work is currently citable by using the Digital Object Identifier (DOI) given below. The VoR will be published online in Early View as soon as possible and may be different to this Accepted Article as a result of editing. Readers should obtain the VoR from the journal website shown below when it is published to ensure accuracy of information. The authors are responsible for the content of this Accepted Article.

**To be cited as:** *Eur. J. Inorg. Chem.* 10.1002/ejic.201700597

**Link to VoR:** <http://dx.doi.org/10.1002/ejic.201700597>

# The Catalytic Properties of Copper-based Nanoscale Coordination Polymer Fabricated by Solvent-Etching Top-Down Route

Xiaowei Cao, Zhenlan Fang, Wei Huang and Qiang Ju\*

**Abstract:** Manipulating particle size is a powerful mean of creating unprecedented applications both in inorganic and organic materials. Coordination polymer, emerging as one sort of organic-inorganic hybrid materials, has attracted thriving interests in a variety of applications, but nanoscale coordination polymer has scarcely been touched. In this work, pure-phase coordination polymer  $[\text{Cu}_6(1,4\text{-bis(imidazol-1-yl)butane)}_3\text{I}_6]_\infty$  with different sizes as well as morphologies was synthesized through facile top-down route assisted with solvent-etching for the first time. The size and morphology could be adjusted just via varying the participated etching solvents. Our mechanistic investigation suggest that the bulk coordination polymer as precursor in the etching solvents may experience a process of dispersion, dissolution, recrystallization to generate the nanoscale counterpart. Higher catalytic activity of nanoscale coordination polymer was observed in N-arylation of imidazole aryl halide, and was attributed to higher surface area and lower coordination number of unsaturated coordination sites (CUSs). This simple and rapid preparation, requiring neither specialized equipment nor harsh conditions, suggests a wealth of potential for reducing down the size of coordination polymer to comply with various practical applications.

## Introduction

The last decade has witnessed rapid developments and innovations in both coordination polymer/metal organic frameworks (CPs/MOFs) and nanotechnology.<sup>[1]</sup> CPs/MOFs are materials consisting of metal ions or clusters coordinated to organic molecules, and have been explored in diverse technical applications, such as heterogeneous catalysis, optical materials, and gas storage.<sup>[2]</sup> Nanoparticles, owing to their small size as well as large surface-to-volume ratio, have also been extensively employed in catalysis, biodetection, lighting, and drug delivery.<sup>[3]</sup> Thus, nanoscale coordination polymer (NCPs), which combine the merits of CPs and nanoparticles, have become one of the hottest topics as their charming properties could address the issues confronted in fundamental researches and technical applications. For example, NCPs have been applied as contrast agents to perform multimodal bioimaging, as vehicle for drug delivery and release, as catalyst in chiral catalysis, and as platform for lighting.<sup>[4]</sup> Most of the reported NCPs were

synthesized with the assistance of surfactant or/and interface, while the synthesis strategy would inevitably demand CPs endowing with fast nucleation rate to make it possible to control the formation of nanoparticles.<sup>[5]</sup> For the CPs with low nucleation rate, it is conducive/necessary to conduct the reaction under high-temperature, high-pressure, time-resuming, and more reactants than obtained products, in order to yield pure CPs with high crystallinity. However, all of these conditions would play detrimental roles in controlling morphology, size, and phase purity of NCPs. Thus, it is urgent to propose one route for generating pure, and monodispersed NCPs with adjustable size.

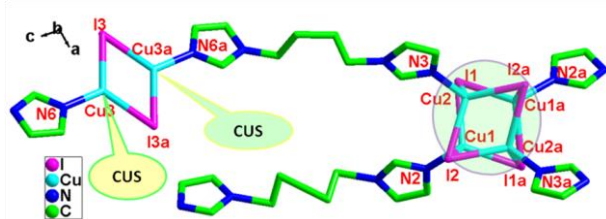
Bottom-up method, which can manipulate the assembly of atoms and/or clusters, may be the most common strategy to fabricate nanoparticles with tunable size, monodispersion, and high-crystallinity.<sup>[6]</sup> Top-down route is performed via using bulk materials as precursor to generate nanoscale counterpart through physical and/or chemical effect shrinking bulk material into nanoscale counterpart, which has also been extensively investigated in the synthesis of nanoparticles.<sup>[7]</sup> In the last decades, shrinking bulk materials into nanometer dimension without the re-assembly of atoms has been found considerable utilization for the preparation of two-dimension nanomaterial (such as graphene nanosheet)<sup>[8]</sup> and ionic liquid solid/frozen nanoparticles.<sup>[9]</sup> However, this way often face the challenges in term of uniformity of obtained nanoparticles. As other type of top-down route, the way of *in situ* dissolve-recrystallize-formation of nanoparticles in appropriate solvents, is anticipated to efficiently manipulate the size of obtained nanoparticles and promise the phase purity of obtained nanoparticles. But to the best of our knowledge, this way has not drawn attention on the controllable synthesis of nanomaterials, not to mention the synthesis of NCPs. In this work, we have utilized a facile solvent-etching top-down route to synthesize pure, uniform and monodispersed NCPs. The size and morphology of obtained NCPs could be modulated by varying applied etching solvents. The generated NCPs could be used as efficient catalysis for the N-arylation of imidazole aryl halide.

## Results and Discussion

**Structure Description.** Bulk CPs  $[\text{Cu}_6(\text{L}1)_3\text{I}_6]_\infty$  (BCPs), which contains two active  $\text{Cu}^{1+}$  and four inactive  $\text{Cu}^{1+}$  ions, were prepared via the self-assembly of ligand L1 [1,4-bis(imidazol-1-yl)butane] with  $\text{CuI}$  under hydrothermal conditions for 24 hours, taken as an example to illustrate the synthesis of nanoscale counterpart (Figure 1).<sup>[10]</sup> Single-crystal X-ray diffraction analysis revealed that BCPs crystallizes in the monoclinic  $C_2/c$  space group and has a corrugated layer configuration (Figure S1). The detailed crystal data as well as the bond length and angles were shown in

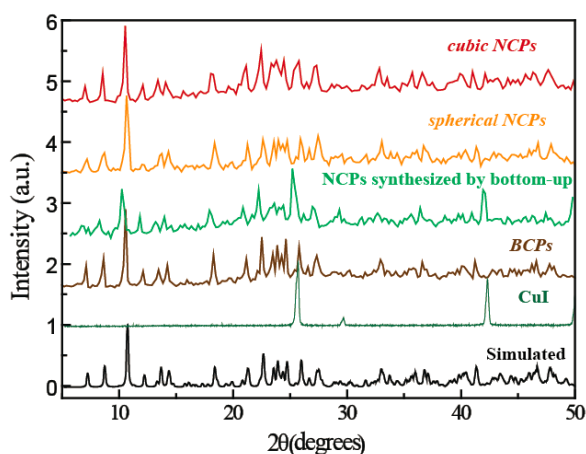
X.W. Cao, Z.L. Fang, W. Huang, Q. Ju  
Key Laboratory of Flexible Electronics (KLOFE) & Institute of Advanced Materials (IAM), Jiangsu National Synergetic Innovation Center for Advanced Materials (SICAM), Nanjing Tech University (NanjingTech), 30 South Puzhu Road, Nanjing 211816, P.R. China.  
E-mail: iamqju@njtech.edu.cn

## Communication



**Figure 1.** Perspective view of coordination environments of Cu and L1 (All hydrogen atoms were omitted for clarity).

Table S1-2. As shown in Figure 1, BCPs possesses functional tetranuclear  $\text{Cu}_4\text{I}_4$  and dinuclear  $\text{Cu}_2\text{I}_2$  clusters simultaneously.  $\text{Cu}_4\text{I}_4$  unit displays a centrosymmetric cubane-like arrangement with Cu(I) and iodide occupying alternate corners of the cube, in which Cu(I) centers are in a distorted tetrahedral geometry and are coordinated by three iodides and one nitrogen atom from bimb (Cu1 and Cu2 in Figure 1). The Cu-Cu separations are 2.72-2.88 Å, which are comparable with those in the reported cubane-like  $\text{Cu}_4\text{I}_4$  analogues.  $\text{Cu}_2\text{I}_2$  unit shows a rhomboidal arrangement, in which Cu(I) centers are in a distorted triangular geometry and are coordinated by two iodides and one nitrogen atom from bimb (Cu3 in Figure 1). The Cu-Cu separation in  $\text{Cu}_2\text{I}_2$  unit is 2.47 Å, which is much shorter than those in the  $\text{Cu}_4\text{I}_4$  unit. With respect to Cu1 and Cu2 (four-coordinated), Cu3 (three-coordinated) can serve as coordination unsaturated site (CUS). The prominent copper-iodine aggregates acting as inorganic building blocks have attracted considerable attentions due to their fascinating and efficient catalysis originating from CUS, such as the formation of C-N bond<sup>[11]</sup> and the azide-alkyne cycloaddition (CuAAC).<sup>[12]</sup> Thus, the obtained BCPs at smaller size may be endowed with good catalysis. Bimb shows *anti-anti-anti* and *anti-gauche-anti* conformations with the twisting angle of two imidazolyl rings in bimb being 86.5° and 87.1°, respectively (Figure S1). The two type of bimb alternatively link  $\text{Cu}_4\text{I}_4$  and  $\text{Cu}_2\text{I}_2$  units into a corrugated layer

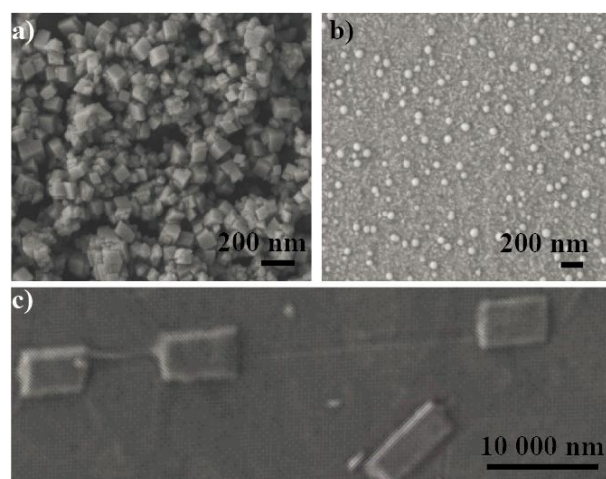


**Figure 2.** XRD patterns of *cubic NCPs* and *spherical NCPs* obtained by top-down route, NCPs synthesized by bottom-up method, BCPs, CuI and the simulated data of BCPs obtained from single-crystals analysis

consisting of metal-organic macrocycles. It should be mentioned that the layers are further interpenetrated to form 1D large channels with the effective dimensions being  $11.26 \times 8.62 \text{ Å}^2$  (Figure S2-3).

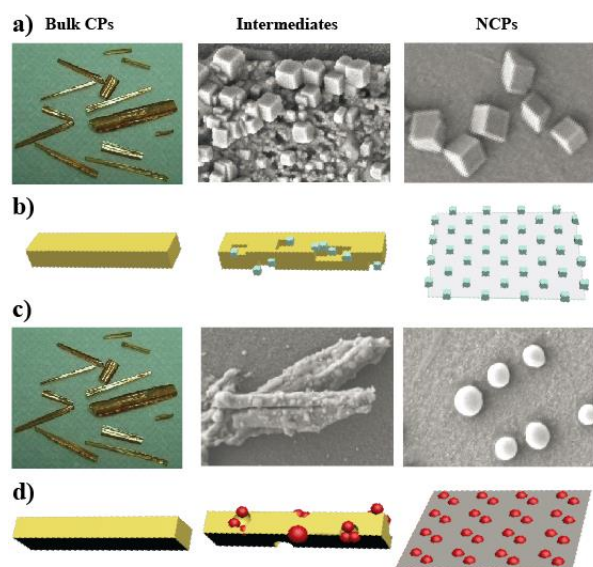
**Synthesis of NCPs.** Two categories of methods, bottom-up and top-down, were adopted to synthesize NCPs, respectively. Firstly, we attempted to synthesize NCPs via common-used bottom-up method arranging atoms and molecules in nanostructures, where CuI and L1 were used as starting materials under hydrothermal condition. The reaction time was reduced to 4 hours, with the addition of polyvinylpyrrolidone (PVP) serving as surfactant to manipulate the nucleation and growth of NCPs. From the powder X-ray diffraction (XRD) results (Figure 2), the obtained material demonstrated diffraction peaks of BCPs, but it was always accompanied with remaining CuI, which cannot be completely run out even under the condition that the ligand was ten times more than that of stoichiometric ratio. Besides, the size of obtained particles was larger than  $100 \mu\text{m}$ , failing to reduce the size down to nanoscale. Therefore, bottom-up method is not suitable for synthesizing this NCPs, indicating that an effective synthesis strategy for fabricating crystalline NCPs is urgent desired.

For the top-down route, BCPs utilized as precursor were processed under solvothermal condition. The bulk crystals were put into etching solvents in a glass vessel, then heated for 2 hours and the obtained resultant microemulsion was finally poured into solvent with floating ice under ultrasound before centrifugation. In stark contrast to the bottom-up method, no trace of CuI was found out in the XRD and the pattern was in accordance with the file simulated from single crystals data, confirming the purity of obtained NCPs (Figure 2). Moreover, different sizes and diverse morphologies could also be generated when different etching solvents participated (Figure 3). The obtained NCPs were



**Figure 3.** SEM images of NCPs obtained by top-down route via the application of different etching solvents: a) ethanol, b) n-butyl acetate, and c) n-butyl chloride, showing that the appropriate selection of etching solvents play an important role in the synthesis of NCPs.

## Communication

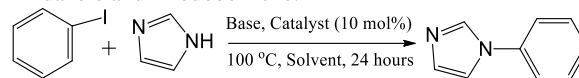


**Figure 4.** SEM images of top-down synthesis NCPs at different stages for a) ethanol, and c) n-butyl acetate, respectively. The proposed fabrication mechanism for b) *cubic NCPs* and d) *spherical NCPs*, respectively.

monodispersed cubic particles with the size to be ~145 nm, when ethanol was selected as solvent (*cubic NCPs*, Figure 3a). Smaller (~91 nm) and spherical particles were observed in SEM image when n-butyl acetate was implemented as solvent (*spherical NCPs*, Figure 3b). The size distribution both of cubic and spherical nanocrystals were demonstrated in Figure S4. Interestingly, much larger particles with quasi-rod shape (4~10  $\mu\text{m}$  in length and ~2  $\mu\text{m}$  in width) were yielded when n-butyl chloride was employed (Figure 3c). These results indicate that the applied solvents played an important role in adjusting size and morphology of NCPs obtained by top-down route. Besides, both *spherical NCPs* and *cubic NCPs* could be dispersed in aqueous solution, which were confirmed by Tyndall effect in their corresponding colloidal suspensions (Figure S5), promising their potential application in biodetection.

**Synthesis Mechanism.** To illustrate the growth mechanism of NCPs via top-down route, the morphologies of particles obtained at different stages were acquired. The starting bulk crystals were quasi-rod with a size in the mm range and demonstrated length to width ratio to be 8~12 (Figure 4), showing larger length-to-width ratio than that of quasi-rod obtained by n-butyl chloride (Figure 3c). This variation indicated that n-butyl chloride preferred to crumble BCPs in the length dimension. When the synthesis procedure of *spherical NCPs* by ethanol lasted for 1 hour (intermediate), cubic particles with different sizes could be clearly observed on the surface of rod-like BCPs (Figure 4a). When the synthesis time extended to two hours, there were only *cubic NCPs* in the yielded products. Similarly, when n-butyl acetate was used as solvent, there were spherical particles with different sizes

**Table 1:** Screening of Reaction Conditions in *N*-arylation of imidazole and 4-iodobenzene.



Entry	Catalyst <sup>a</sup>	Base	Solvent	Yield(%) <sup>b</sup>
1 <sup>c</sup>	BCPs	K <sub>2</sub> CO <sub>3</sub>	DMF	41
2	BCPs	KOH	DMF	50
3	BCPs	NEt <sub>3</sub>	DMF	Trace
4 <sup>d</sup>	BCPs	Cs <sub>2</sub> CO <sub>3</sub>	H <sub>2</sub> O	28
5	BCPs	Cs <sub>2</sub> CO <sub>3</sub>	THF	28
6	CuI	Cs <sub>2</sub> CO <sub>3</sub>	DMF	68
7 <sup>e</sup>	CuI and bimb	Cs <sub>2</sub> CO <sub>3</sub>	DMF	78
8	BCPs	Cs <sub>2</sub> CO <sub>3</sub>	DMF	95
9	<i>Cubic NCPs</i>	Cs <sub>2</sub> CO <sub>3</sub>	DMF	100
10	<i>Spherical NCPs</i>	Cs <sub>2</sub> CO <sub>3</sub>	DMF	100

<sup>a</sup> Reaction conditions: iodobenzene (0.5 mmol), imidazole (0.75 mmol), base (0.1 mmol), Cu source (0.05 mmol), solvent (2.0 mL), 100 °C, 24 h, under N<sub>2</sub>; <sup>b</sup> GC yields; <sup>c</sup> Average of two runs; <sup>d</sup> 0.5 mmol tetrabutyl ammonium bromide (TBAB) was added as additive; <sup>e</sup> bimb as a ligand with the molar ratio of CuI:bimb is 2:1.

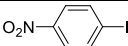
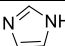
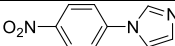
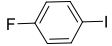
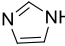
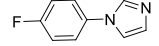
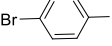
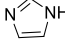
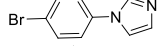
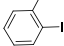
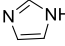
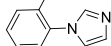
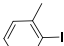
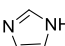
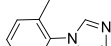
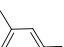
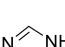
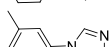
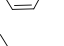

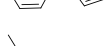
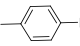
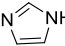
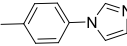
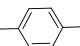
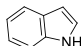
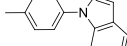
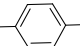
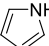
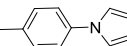
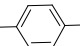
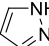
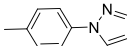
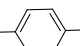
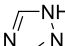
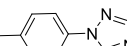
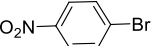
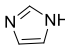
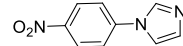
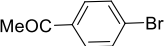
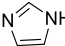
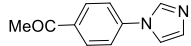
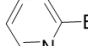
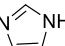
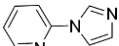
attached on the rod-like BCPs in the intermediate and spherical particles were presented in the final obtained nanoparticles (Figure 4c). Both of the morphologies of these intermediates are in accordance with the final obtained nanoparticles. Based on these results, the plausible formation mechanism of NCPs is proposed. Firstly, the bulk crystal could be partially dissolved to generate supersaturated micro-emulsion in appropriate solvents under appropriate temperature and pressure, accompanied with *in-situ* generated small nanoparticles. Secondly, more uniform NCPs were yielded when this dissolve-recrystallization reached equilibrium. The *in situ* generation and formation of NCPs should be the key point for yielding pure and uniform NCPs without impurity. While for the modulation of morphology and size of yielded nanoparticles, it should be determined by the polarity of applied etching solvents.

**Catalysis.** Aforementioned analysis on the structure has pointed out that the rhomboid geometry centrosymmetric [(Cu<sub>3</sub>)<sub>2</sub>(I<sub>3</sub>)<sub>2</sub>] clusters may enable BCPs with catalysis activity. Taken the small size of NCPs into account, its catalytic activity and stereoselectivity would be greatly improved, as high surface area can implement high possibility for substrates to access catalytically active sites. To this end, the catalysis behavior of BCPs and NCPs on the *N*-arylation of imidazole aryl halide has



## Communication

**Table 2.** Scope of *N*-arylation of imidazole and halide-benzene reactions catalyzed by *cubic NCPs*

Entry	Ar-X	Nucleophile	Product <sup>a</sup>	Yield(%) <sup>b</sup>
1				100(96)
2				100(88)
3				100(92)
4				43
4 <sup>c</sup>				45
5				75
5 <sup>d</sup>				78
6				83
7				55
8				100(97)
9				100(97)
10				100(88)
11				100(95)
12				40
13				77

<sup>a</sup> Reaction conditions: aryl halide (0.5 mmol), imidazole (0.75 mmol), Cs<sub>2</sub>CO<sub>3</sub> (0.1 mmol), *cubic NCPs* (0.05 mmol), DMF (2.0 mL), 100 °C, 24 h, under N<sub>2</sub>; <sup>b</sup> GC yields; <sup>c</sup> the spherical NCPs was used as catalyst; <sup>d</sup> the spherical NCPs was used as catalyst. Isolated yields are given in parentheses.

been performed. BCPs were chosen as catalyst to firstly optimize the reaction condition. As shown in Table 1, this cheap, air-stable BCPs catalyst was active in promoting Ullmann *N*-arylation by achieving a high conversion of iodobenzene up to 95%, where Cs<sub>2</sub>CO<sub>3</sub> was used as a base in *N,N*-dimethylformamide (DMF). Importantly, compared with BCPs, the yields of products for *cubic* and *spherical NCPs* have been improved and reach as high as 100%. This should be induced by the relative high surface to volume ratio, bringing out more accessible coordination unsaturated sites (CUSs) as well as lower coordination number of surface CUSs, normally terminated by vacancies.<sup>[13]</sup>

Under the above-optimized conditions of *N*-arylation with imidazole, the catalysis effect of varying aryl halides was also investigated on *cubic NCPs* (Table 2). The aryl iodides bearing electron-withdrawing groups, such as -NO<sub>2</sub>, -F and -Br, provided the desirable products in a quantitative yield (~100%, entry 1, 2 and 3, respectively). However, moderate yields were observed for aryl iodides with electron-donating groups, such as -Me (43%, 75%, 83%, entry 4, 5, 6, respectively). These results are

consistent with the well-established trend in Cu-catalyzed Ullmann reactions.<sup>[14]</sup> The yield of arylation of imidazole with 2-, 3- or 4- iodotoluene reduced in turn, which could be ascribed to the steric effect of the methyl group (entries 4-6). It should be pointed out that the *spherical NCPs* show similar catalysis efficiency when they were used in entries 4-5 in contrast to *Cubic NCPs*. Interestingly, except imidazole, other azoles such as pyrrole (entry 8), pyrazole (entry 9) and triazoles (entry 10) could also couple with 4-iodotoluene to produce the target product in moderate condition to an excellent yield (~100%). Due to the steric hindrance, imidazole (83%, entry 6) was proved to be more reactive than indole (55%, entry 7), much less reactive than pyrazole, pyrrole and triazole (~100%, entries 8-10). Arylation of imidazole and aryl bromide containing the electron-withdrawing groups (-NO<sub>2</sub>) can be carried out with desirable products in a high yield (~100%, entry 11). Noticeably, arylation of imidazole can even take place with aryl bromide bearing electron-donating group (-COMe) (~40%, entry 12) in an acceptable yield, and with the heteroaromatic 2-bromopyridine afforded the desirable

## Communication

products in a satisfactory yield (77%, entry 13). In order to check the reusability and stability of the NCPs catalysts, the reaction of azide-alkyne cycloaddition was chosen as model (Table S3). The yield of cubic and spherical NCPs show the yield to be 100%, which is higher than that of BCPs (90%). As shown in Figure S6, the reaction of NCPs could finish the experiment in 20 hour with the yield to be 100%, further demonstrating the better catalysis of NCPs. Especially, after four runs, the yield of product was still high up to 88%. The XRD pattern of cubic NCPs after catalysis reaction maintains as well as the starting one, demonstrating the reusability and stability of NCPs.

## Conclusions

In summary, we have firstly proposed a solvent-etching top-down route for the fabrication of NCPs. The *cubic* and *spherical* NCPs could be generated by selecting appropriate etching solvents and using BCPs as precursor under mild experiment conditions. Different with the bottom-up route, no impurity were observed in the obtained sample of solvent-etching top-down route. The intrinsic advantage of CPs in catalysis has been further strengthened when they combined with smaller size, and the *cubic* NCPs have been demonstrated as efficient catalyst for Ullmann N-arylation. This work may open the door for the facile synthesis and catalysis application of NCPs.

## Acknowledgements

This work was financially supported by National Basic Research Program of China (973 Program, No. 2015CB932200), National Natural Science Foundation of China (61136003, 51173081, 21501089 and 61505077), Natural Science Foundation of Jiangsu Province, China (BM2012010, BK20150936 and BK20150939).

**Keywords:** Coordination Polymer, Nanomaterials, Catalysis, Top-Down

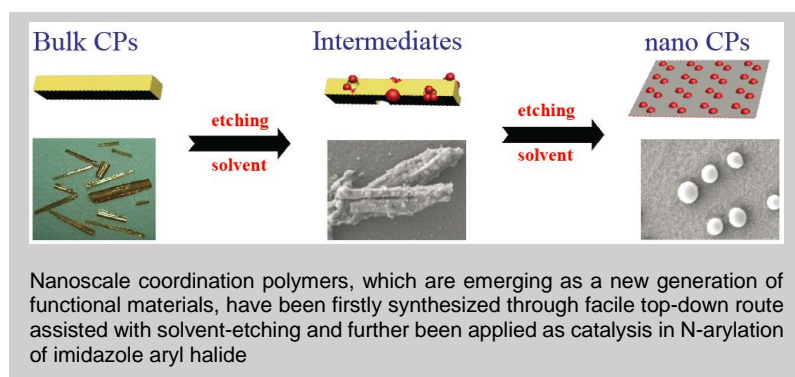
- [1] a) C. He, D. Liu, W. Lin, *Chem. Rev.* **2015**, *115*, 11079; b) M. Sindoro, N. Yanai, A.-Y. Jee, S. Granick, *Acc. Chem. Res.* **2014**, *47*, 459; c) P. Mahato, A. Monguzzi, N. Yanai, T. Yamada, N. Kimizuka, *Nature Mater.* **2015**, *14*, 924; d) Q. H. Yang, Y. Z. Chen, Z. Y. U. Wang, Q. Xu, H. L. Jiang, *Chem. Commun.* **2015**, *51*, 10419.
- [2] a) Q.-L. Zhu, Q. Xu, *Chem. Soc. Rev.* **2014**, *43*, 5468; b) Y. Cui, B. Chen, G. Qian, *Coord. Chem. Rev.* **2014**, *273*, 76; c) J. W. Zhang, H. T. Zhang, Z. Y. Du, X. Q. Wang, S. H. Yua, H. L. Jiang, *Chem. Commun.* **2014**, *50*, 1092; d) S. Hermes, T. Witte, T. Hikov, D. Zacher, S. Bahnmueller, G. Langstein, K. Huber, R. A. Fischer, *J. Am. Chem. Soc.* **2007**, *129*, 5324; e) Z.-W. Wei, C.-X. Chen, S.-P. Zheng, H.-P. Wang, Y.-N. Fan, Y.-Y. Ai, M. Pan, C.-Y. Su, *Inorg. Chem.* **2016**, *55*, 7311; f) T. Yang, H. Cui, C. Zhang, L. Zhang, C.-Y. Su, *Inorg. Chem.* **2013**, *52*, 9053.
- [3] P. Zrazhevskiy, M. Sena, X. H. Gao, *Chem. Soc. Rev.* **2010**, *39*, 4326.
- [4] a) T. Baati, L. Njim, F. Neffati, A. Kerkeni, M. Bouttemi, R. Gref, M. F. Najjar, A. Zakhama, P. Couvreur, C. Serre, P. Horcajada, *Chem. Sci.* **2013**, *4*, 1597; b) T. Rodenas, I. Luz, G. Prieto, B. Seoane, H. Miro, A. Corma, F. Kapteijn, F. X. L. I. Xamena, J. Gascon, *Nature Mater.* **2015**, *14*, 48; c) Y. Lu, B. Yan, *Chem. Commun.* **2014**, *50*, 13323; d) B. J. Yao, W. L. Jiang, Y. Dong, Z. X. Liu, Y. B. Dong, *Chem. Eur. J.* **2016**, *22*, 10565; e) Y. Jiang, X. Zhang, X. Dai, W. Zhang, Q. Sheng, H. Zhuo, Y. Xiao, H. Wang, *Nano Res.* **2017**, *10*; f) B. Rungtaweeworanit, Y. Zhao, K. M. Choi, O. M. Yaghi, *Nano Res.* **2016**, *9*, 45.
- [5] a) J. Della Rocca, D. M. Liu, W. B. Lin, *Acc. Chem. Res.* **2011**, *44*, 957; b) P.-Z. Li, Y. Maeda, Q. Xu, *Chem. Commun.* **2011**, *47*, 8436.
- [6] C. B. Murray, D. J. Norris, M. G. Bawendi, *J. Am. Chem. Soc.* **1993**, *115*, 8706.
- [7] W. J. Roth, P. Nachtigall, R. E. Morris, P. S. Wheatley, V. R. Seymour, S. E. Ashbrook, P. Chlubna, L. Grajciar, M. Polozij, A. Zukal, O. Shvets, J. Cejka, *Nature Chem.* **2013**, *5*, 628.
- [8] Y. X. Wang, M. T. Zhao, J. F. Ping, B. Chen, X. H. Cao, Y. Huang, C. L. Tan, Q. L. Ma, S. X. Wu, Y. F. Yu, Q. P. Lu, J. Z. Chen, W. Zhao, Y. B. Ying, H. Zhang, *Adv. Mater.* **2016**, *28*, 4149.
- [9] A. Tesfai, B. El-Zahab, D. K. Bwambok, G. A. Baker, S. O. Fakayode, M. Lowry, I. M. Warner, *Nano Lett.* **2008**, *8*, 897.
- [10] D. Sun, S. Yuan, H. Wang, H. F. Lu, S. Y. Feng, D. F. Sun, *Chem. Commun.* **2013**, *49*, 6152.
- [11] a) G. Evano, N. Blanchard, M. Toumi, *Chem. Rev.* **2008**, *108*, 3054; b) F. Monnier, M. Taillefer, *Angew. Chem. Int. Ed.* **2008**, *47*, 3096; c) I. P. Beletskaya, A. V. Cheprakov, *Coord. Chem. Rev.* **2004**, *248*, 2337.
- [12] a) M. Meldal, C. W. Tornoe, *Chem. Rev.* **2008**, *108*, 2952; b) A. Dondoni, *Chem-Asian J* **2007**, *2*, 700; c) J. F. Lutz, *Angew. Chem. Int. Ed.* **2007**, *46*, 1018; d) T. S. A. Hor, F. W. Li, *Chem-Eur J* **2009**, *15*, 10585; e) J. E. Moses, A. D. Moorhouse, *Chem. Soc. Rev.* **2007**, *36*, 1249.
- [13] a) Z. Fang, B. Bueken, D. E. De Vos, R. A. Fischer, *Angew. Chem. Int. Ed.* **2015**, *54*, 7234; b) Z. L. Fang, J. P. Durholt, M. Kauer, W. H. Zhang, C. Lochenie, B. Jee, B. Albada, N. Metzler-Nolte, A. Poppl, B. Weber, M. Muhler, Y. M. Wang, R. Schmid, R. A. Fischer, *J. Am. Chem. Soc.* **2014**, *136*, 9627.
- [14] J. Hassan, M. Sevignon, C. Gozzi, E. Schulz, M. Lemaire, *Chem. Rev.* **2002**, *102*, 1359.

## Communication

Entry for the Table of Contents (Please choose one layout)

Layout 1:

## FULL PAPER

**The Catalytic Properties of Copper-based Nanoscale Coordination Polymer Fabricated by Solvent-Etching Top-Down Route***Xiaowei Cao, Zhenlan Fang, Wei Huang and Qiang Ju\**

\*nanoscale coordination polymer